TECHNICAL PAPER
Journal of the South African Institution of Civil Engineering, 44(2) 2002,
Pages 14–22, Paper 509

The use of the correspondence principle towards the fatigue characterisation of asphalt concrete

N E Galé and A T Visser

Prediction of the performance of asphalt concrete under realistic traffic conditions needs a sound understanding of the hysteretic stress-strain behaviour of asphalt concrete mixtures under repetitive traffic loading. Fatigue cracking caused by repetitive traffic loading is one of the major distresses in asphalt concrete pavement. The most common fatigue model relates the initial strain or stress levels applied during tests to the fatigue life, without taking into account damage evolution. As a result, this fatigue model grossly underpredicts field fatigue life and the introduction of laboratory to field shift factors is necessary.

The aim of this paper is, therefore, to introduce a methodology capable of predicting the fatigue performance of asphalt concrete considering damage evolution. Other aspects, such as difference in loading, the changing field environmental conditions, as well as different support conditions, which also necessitate the introduction of shift factors, fall outside the scope of the present research.

The correspondence principle was used to achieve this objective, owing to its ability to separately evaluate the three major mechanisms that take place in the asphalt concrete when subjected to repetitive loading with various durations of rest periods: fatigue, which can be regarded as damage accumulation due to flow and crack propagation, relaxation of stresses, related to the viscoelastic nature of asphalt concrete, and chemical healing, across microcrack and macrocrack interfaces, during rest periods. Furthermore, the correspondence principle was used to derive a constitutive equation where damage mechanisms were accounted for. Finally, a fatigue prediction curve was derived, based on this constitutive modelling approach. As a result, a higher fatigue life, in terms of number of load applications to failure, was obtained by using this methodology, indicating more realistic fatigue life prediction and less necessity for the use of shift factors. This paper is based on the MEng project report submitted to the University of Pretoria by the first author, titled 'Fatigue characterization of asphalt concrete using viscoelasticity and damage theory'.

NELSON GALÉ qualified as a civil engineer in Argentina and immigrated to South Africa in 1991. He worked as a site engineer for a civil engineering contractor and later joined the Johannesburg City Council. From 1995 he was involved in the design of road and stormwater drainage systems for the Western Metropolitan Local Council. In 1998 he joined a consultant company in Pretoria where he participated in the design of the Maputo Development Corridor. He was registered as a professional engineer with ECSA in 1998. His academic qualifications include an MEng (Transportation Engineering) from the University of Pretoria. At present he works for Jeffares and Green Inc in the fields of rehabilitation and materials engineering.

ALEX VISSER is the SA Roads Board Professor in Transportation Engineering in the Department of Civil Engineering at the University of Pretoria. He holds the degrees BSc(Eng) (Cape Town), MSc(Eng) (Wits), PhD(University of Texas at Austin) and BComm(SA). His fields of research interest are primarily low-volume road design and maintenance, roads for ultra-heavy applications, and road management systems. He is a fellow and past president of the South African Institution of Civil Engineering (SAICE) and serves on the SAICE Council. In 1998 he was awarded the SAICE Award for Meritorious Research for his contributions to low-volume road technologies.

INTRODUCTION

Accurate prediction of the fatigue performance of asphalt concrete under complex traffic loading conditions is extremely difficult, and there is a continuous search for improved techniques. The aim of this paper is to present an approach which has the potential to realistically predict fatigue life by using the correspondence principle and also to demonstrate its applicability by deriving a constitutive equation which, in turn, is used to obtain a fatigue curve for continuously graded asphalt.

Three major mechanisms take place in asphalt concrete when it is subjected to repetitive traffic loading: *fatigue, relaxation of stresses* and *chemical healing* (Kim *et al* 1995). Fatigue is a damage mechanism that degrades pavement performance, whereas relaxation and healing mechanisms increase the life of asphalt concrete pavement. To accurately evaluate the response of asphalt concrete under traffic loading, a sound understanding of these mechanisms is required. As these mechanisms occur simultaneously, the evaluation is complicated. A methodology based on the use of the correspondence principle allows the separate evaluation of these three major mechanisms. Consequently, an experimental approach to verify the correspondence principle was followed in this study based on a series of constant-strain-rate monotonic loading laboratory tests.

CORRESPONDENCE PRINCIPLE

Theoretical framework

The time-dependent behaviour of asphalt mixes is illustrated in figure 1. Stresses due to a cyclic strain history (fig 1(a)) are calculated from a linear viscoelastic constitutive equation for the uniaxial loading condition with a typical relaxation modulus of asphalt concrete. The equation used is as follows (Kim *et al* 1996):

$$\sigma = \int_0^t E(t-\tau)\frac{d\varepsilon}{d\tau}d\tau \quad (1)$$

where

$E(t)$ = relaxation modulus
σ = uniaxial stress
ε = uniaxial strain

The resulting stress-strain behaviour presents hysteresis loops even though there is no damage induced in the material.

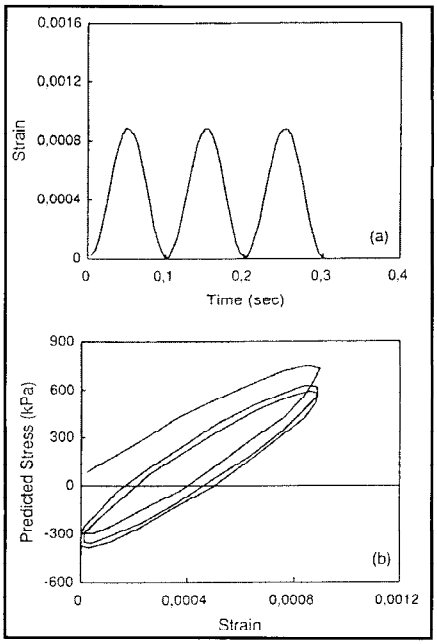

Figure 1 Stress-strain behaviour of a typical asphalt mix obtained from a viscoelastic constitutive relationship: (a) strain input; (b) predicted stress-strain behaviour (after Kim et al 1996)

The theory of viscoelasticity allows viscoelastic problems to be transformed so that they are mathematically equivalent to those for elastic problems with the substitution of elastic moduli. This correspondence can be made by taking appropriate transformation of the elastic governing field and boundary equations of viscoelastic problems with respect to time.

Schapery (1984) proposed an elastic-viscoelastic correspondence principle that can be applicable to both linear and nonlinear viscoelastic materials. He suggested that constitutive equations for certain viscoelastic media are identical to those for the elastic cases, but stresses and strains are not necessarily physical quantities in the viscoelastic body but instead they are pseudo variables in the form of convolution integrals such as:

$$\varepsilon_{ij}^R = \frac{1}{E_R}\int_0^t E(t-\tau)\frac{\delta\varepsilon_{ij}}{\delta\tau}d\tau \quad (2)$$

$$\sigma_{ij}^R = E_R\int_0^t D(t-\tau)\frac{\delta\sigma_{ij}}{\delta\tau}d\tau \quad (3)$$

where

$\sigma_{ij}, \varepsilon_{ij}$ = physical stresses and strains
$\sigma_{ij}^R, \varepsilon_{ij}^R$ = pseudo stresses and strains
E_R = reference modulus
$E(t)$ = relaxation modulus
$D(t)$ = creep compliance

For the case of a growing traction boundary surface, such as crack growth, the viscoelastic problem can be transformed to an elastic case by using physical stresses and strains.

For linear viscoelastic materials, a uniaxial stress-strain relationship, as also presented in equation 1, is

$$\sigma = \int_0^t E(t-\tau)\frac{d\varepsilon}{d\tau}d\tau \quad (4)$$

Using the definition of pseudo strain in equation 2, equation 4 can be expressed as follows:

$$\sigma = E_R\varepsilon^R \quad (5)$$

where

$$\varepsilon^R = \frac{1}{E_R}\int_0^t E(t-\tau)\frac{\delta\varepsilon}{\delta\tau}d\tau \quad (6)$$

A correspondence can be found between equation 5 and the linear elastic stress-strain relationship.

Experimental verification of the correspondence principle

Material and specimen fabrication

The material used in the present study was continuously graded asphalt concrete. The characteristics of the medium grade mix as taken at the asphalt plant are presented in table 1.

The hot mix was compacted at the CSIR Transportek laboratories as a rectangular slab, and cylindrical specimens with a diameter of 100 mm and a height of 110 mm were cored in a horizontal direction perpendicular to the compaction force, consistent with the direction of tensile stress/strain developed near the bottom of an asphalt layer in actual pavement systems. The material used for making the slab was also tested and the density achieved at the laboratory was taken as 2 333 kg/m^3.

The maximum theoretical relative density and the void percentage of the mixture were measured at 2 440 kg/m^3 and 4,4 %, respectively. These results are slightly different from the ones obtained at the plant, but these differences are not meaningful.

Master creep compliance curve

The correspondence principle calls for the calculation of pseudo strains as discussed in the previous section. Calculation of pseudo strains requires the expression of relaxation modulus as a function of time. The relaxation modulus test is extremely difficult to perform and for practical purposes it is desirable to predict the relaxation modulus from a simpler test, such as the creep test.

Therefore, a series of indirect tensile creep tests were performed at three different temperatures (10°C, 25°C and 40°C) in order to obtain the basic thermoviscoelastic properties of the asphaltic mate-

Table 1 Characteristics of the medium grade mix determined at the plant

Type bitumen			60/70 Penetration grade
Bitumen content (%)			5,48
Compacted density (CDM) (kg/m^3)			2 340
Rice SG density (kg/m^3)			2 458
Stability (kN)			10,9
Flow (mm)			3,3
Void percentage			4,8
Grading analysis	**Sieve size (mm)**	**Passing (%)**	**Specification**
	13,2	100	100
	9,5	97	90–100
	6,7	77	69–79
	4,75	60	53–63
	2,36	40	35–45
	1,18	27	27–35
	0,60	20	19–27
	0,30	15	12–20
	0,15	10	7–13
	0,075	6,4	4,7–7,7

Table 2 Indirect tensile creep tests

Number	Temperature (°C)	Load level (kN)	Diameter (mm)	Height (mm)
1	10	1,60	100	110
2	25	1,10	100	110
3	40	0,55	100	110

rial, including the linear viscoelastic relaxation modulus and the time-temperature shift factors required to generate the master creep curve, as discussed below. The indirect tensile creep tests were performed as indicated in table 2.

The creep curves obtained at 10°C, 25°C and 40°C are presented in figure 2. The individual creep curves in figure 2 were then used to construct a master creep curve shown in figure 3. The master creep curve was generated by shifting each individual curve obtained at different temperatures in the horizontal direction on a log-log plot. The dependence of the material property on both time and temperature can be represented by dependence on a single variable, the *reduced time*, and the feature is often referred to as *time-temperature superposition* (Ferry 1980).

It had been observed that time-temperature superposition applies to asphalt concrete at low strain/stress levels (Kim *et al* 1995). In mathematical notation:

$$D(t, T) = DM(\xi) \qquad (7)$$

where DM (ξ) is the master creep function corresponding to a certain *reference temperature* and ξ is *reduced* time defined as

$$\xi = \int_0^t \frac{d\tau}{aT} \qquad (8)$$

where aT is the time-temperature *shift factor*, which is a temperature-dependent material parameter that reflects the influence of temperature on the internal viscosity of the material (Ferry 1980). For a constant temperature, equation 8 reduces to

$$\xi = \frac{t}{aT} \qquad (9)$$

The different shift factors were obtained by measuring the horizontal distance by which each curve in figure 2 shifts to form a master curve, as shown in figure 3, and is illustrated schematically in figure 4.

The temperature of 25°C was selected as the reference temperature for the master curve, and thus the creep compliance curve at this temperature was fixed in time ($aT = 1$ for T = 25°C). Each of the remaining creep compliance curves will thus have a shift factor (aT) associated with it. Figure 5 presents the time-temperature shift factor data and their associated linear fit.

Now, an analytical expression of the master creep function is required and may be obtained by fitting an appropriate mathematical representation such as the *Prony series representation*, discussed in the following section.

The required master relaxation function can then be obtained by converting the master creep function using their interrelationship based on the theory of viscoelasticity.

Hereinafter, the room temperature (T = 25°C) will be taken as the reference temperature and the reduced time will be denoted by t and the master creep function D_M (ξ) and the master relaxation function E_M (ξ) will be denoted by $D(t)$ and $E(t)$, respectively, for notational brevity.

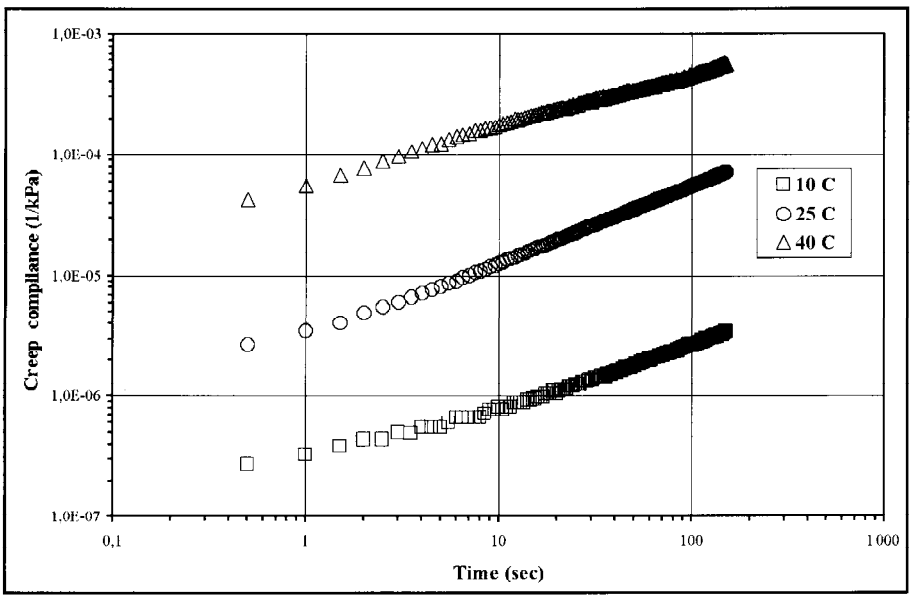

Figure 2 Creep compliance curves at 10°C, 25°C and 40°C

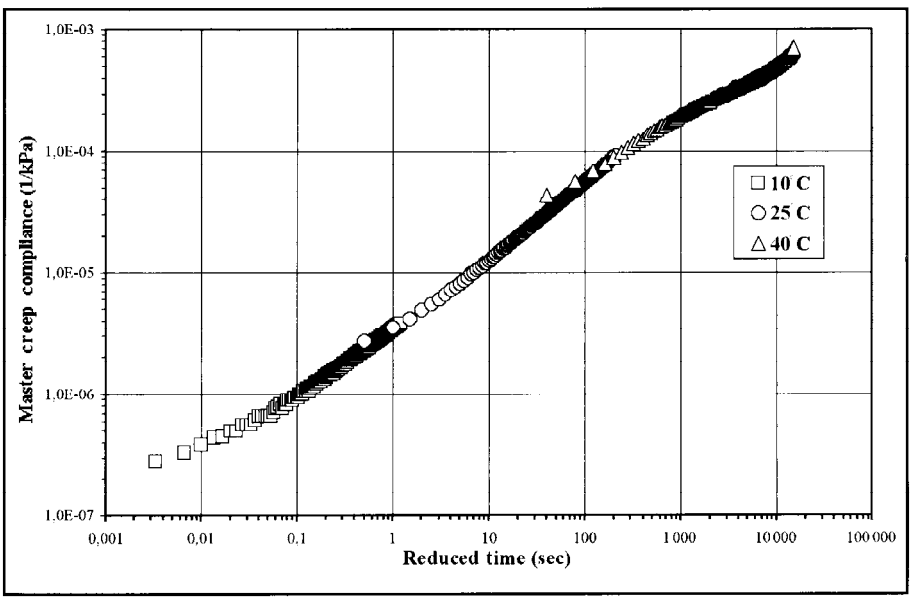

Figure 3 Master creep compliance curve at reference temperature of 25°C

Prony series representation for master creep compliance curve and master relaxation curve

A Prony series representation is widely used in analytically representing linearly viscoelastic behaviours. For instance, for the creep compliance of a linear viscoelastic solid, the following form of representation is used (Park & Kim 1999):

$$D(t) = D_g + \sum_{i=1}^{N} D_i (1 - e^{-\frac{t}{\tau_i}}) \qquad (10)$$

where D_g, D_i, and τ_i are all constants often referred to as the *glassy compliance*, *retardation strength*, and *retardation time*, respectively. Here, the glassy compliance refers to the short-time behaviour of the creep compliance, that is,

$$D_g = \lim_{t \to o} D(t)$$

The series expression equation 10 is based on a mechanical model, commonly referred to as the *generalised Voigt model*, which comprises linear springs and dashpots connected in a particular fashion.

The advantages of the Prony series representation are due to its ability to describe a wide range of viscoelastic responses and the computational efficiency associated with its exponential basis functions.

The *collocation method* was used to fit a Prony series to the given data depicted in figure 3. In the collocation method, the series expression in equation 10 is equated to the data at N different values of the argument (or time), and the N unknowns, Di $(i = 1,...,N)$, are found by solving the resulting system of N linear algebraic equations. Retardation times, τ_i's, are determined *a priori*.

The resulting fit is shown in figure 6. It can be seen that the curve is not quite smooth but slightly wavy. This waviness is mainly due to the influence of local irregularities in the data from experimental noise and an imperfect realisation of the ideal time-temperature superposition.

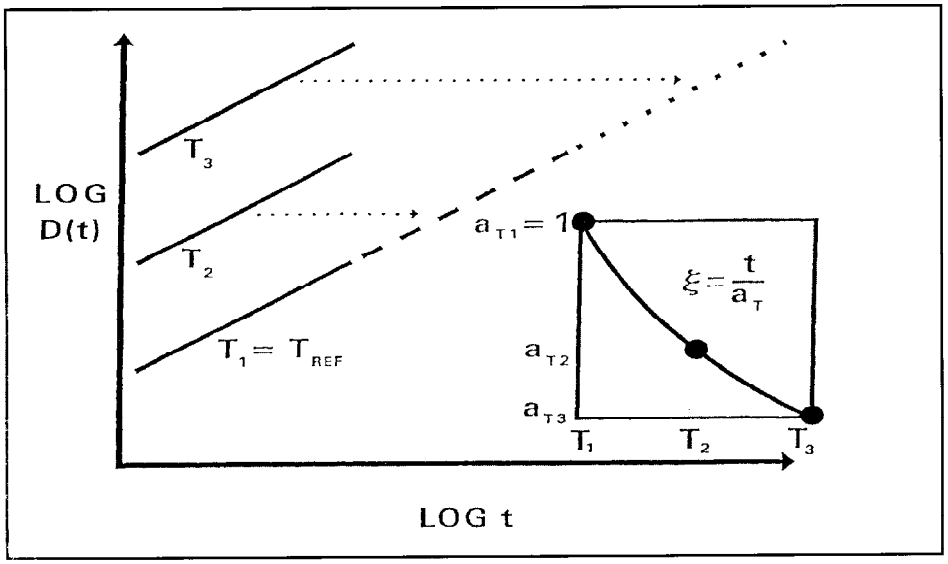

Figure 4 Illustration of the formation of a master creep compliance curve (after Lytton et al 1993)

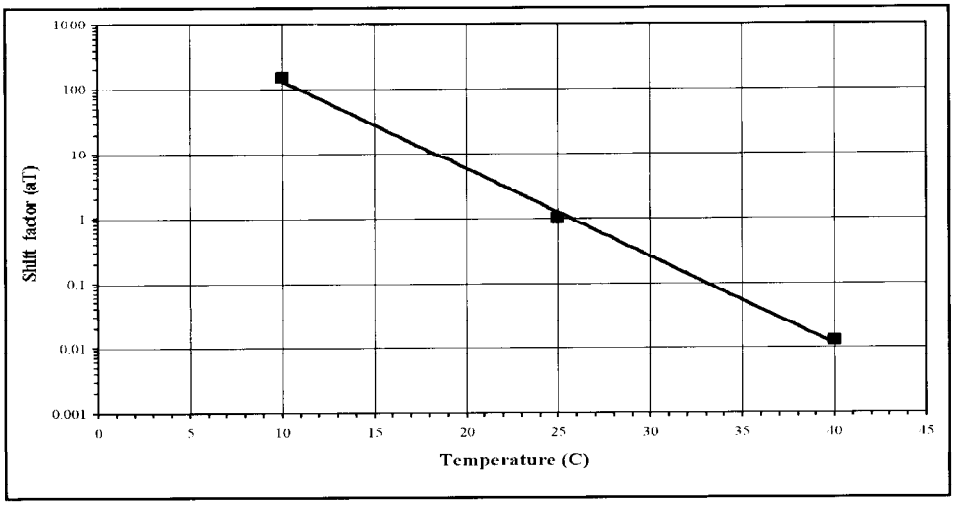

Figure 5 Time-temperature shift factor data and linear fit

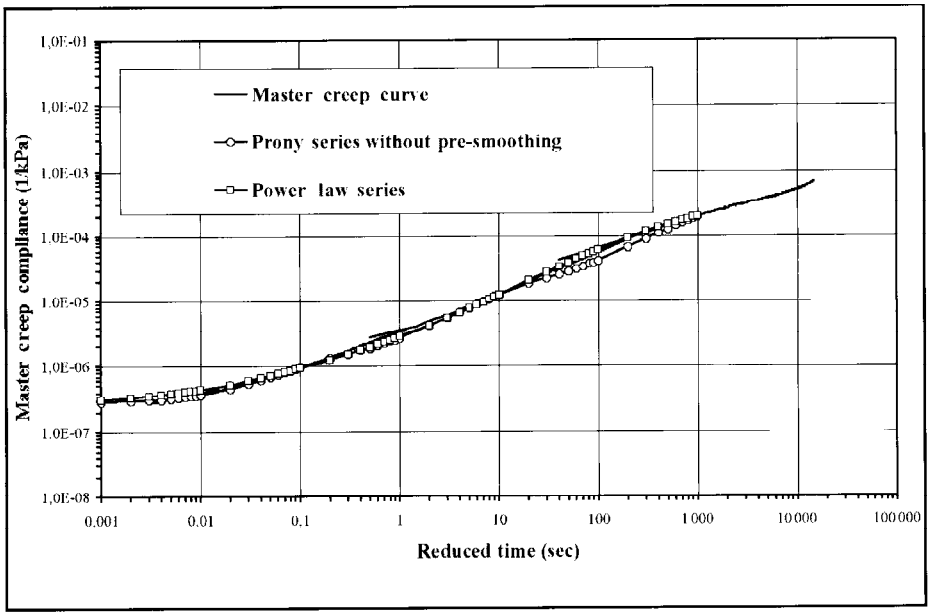

Figure 6 Curve fitting to the master creep curve

It is therefore desirable to pre-mooth the experimental data via an appropriate broadband analytical representation and then find a Prony series representation by fitting it to the smoothed data.

Different methods may be considered for smoothing scattered data and developing a representative curve. A key to this operation is averaging the scattered data so that the resulting curve correctly represents the overall trend of the data without local biases.

In an effort to find such a representation for the experimental creep data given in figure 3, *a power-law series* of the following form was considered (Park & Kim 1999):

$$D(t) = D_g + \sum_{i=1}^{M} \frac{D_i}{(1+\frac{\tau_i}{t})^n} \qquad (11)$$

where Dg , Di , τi , n, and M are all constants. Here, Dg denotes the glassy compliance as in equation 10.

As in the case of the *Prony series fit*, τ_i's can be specified *a priori* and only D_i's are determined by solving the resulting system of M linear equations.

Dg is obtained directly from the glassy behaviour and the exponent n is usually estimated from the slope of the transition zone of the creep curve. In this case, Dg was taken to be equal to 2,76962E-07 kPa^{-1} and n equal to 0,65. A power-law series representation with M = 3 was considered, and the resulting reconstructed creep curve is also plotted in figure 6.

Now, the required master relaxation curve can be obtained by converting the master creep compliance curve function, using their interrelationship based on the theory of linear viscoelasticity (Ferry 1980). According to Ferry, the modulus E(t) is approximately 1/D(t), so that the logarithmic plots have roughly the appearance of mirror images reflected in the time axis. The master relaxation curve is depicted in figure 7 and the mirror effect can be observed if compared with figure 6.

It is now desirable to obtain a Prony series representation of the experimental data which has been pre-smoothed via a power-law series representation. It was pointed out earlier that a direct fit of a Prony series to unsmoothed data with large scatter leads to a problem of local waviness and negative coefficients, which is physically unrealistic. A new, improved Prony series fit to the experimental data was obtained using the following mathematical expression (Park & Kim 1999):

$$E(t) = E_\infty + \sum_{i=1}^{N} E_i \; e^{-t/\rho_i} \qquad (12)$$

Where E_∞, Ei and ρ_i are all constants. The quantity E_∞ in equation 12 is the long-time equilibrium modulus and ρ_i are relaxation times.

It can be seen in figure 7 that the new curve represents the experimental data much better without local waviness. The three-term power-law series representation M = 3 was used in generating the smoothed data. The new Prony series fit was indistinguishable from the parent three-term power-law series representation.

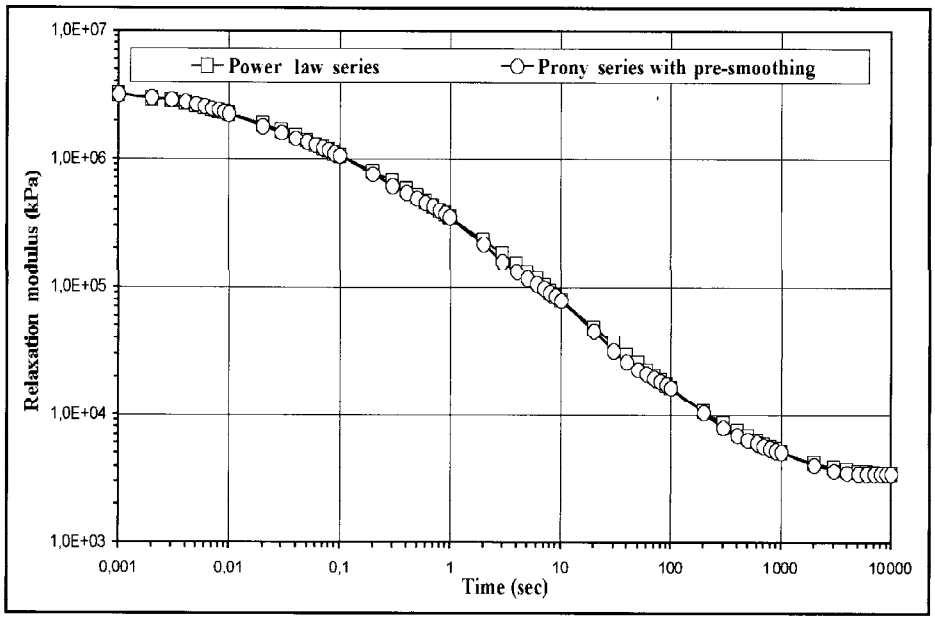

Figure 7 Master relaxation curve at reference temperature of 25°C

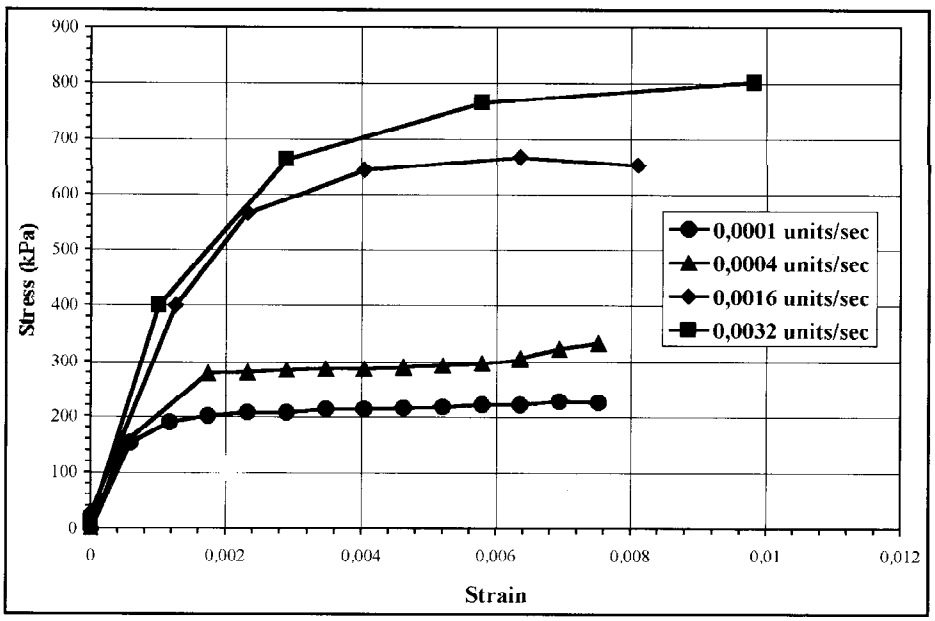

Figure 8 Constant-strain monotonic loading test, stress-strain curves at 0,0001 units/sec, 0,0004 units/sec, 0,0016 units/sec and 0,0032 units/sec

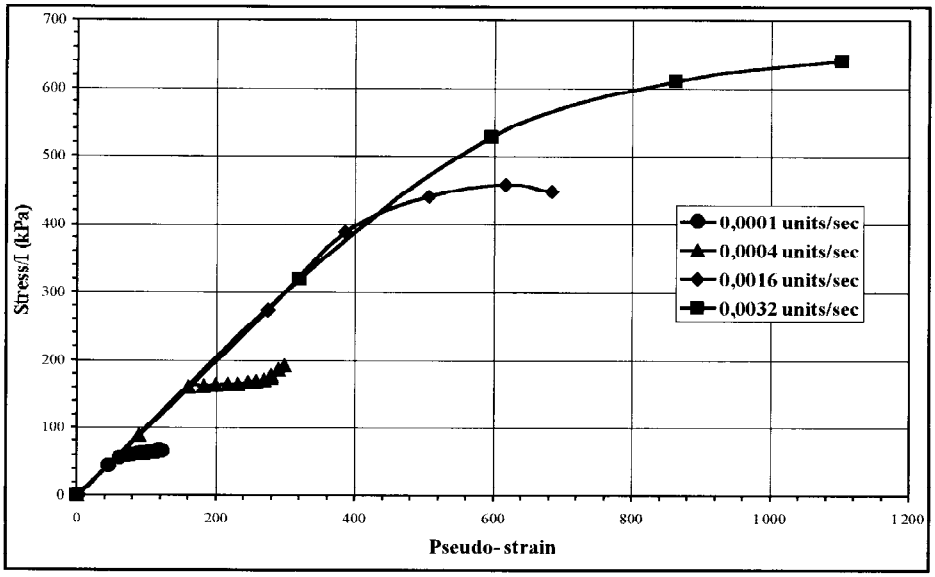

Figure 9 Uniaxial stress-pseudo strain behaviour at different strain rates

APPLICATION OF THE CORRESPONDENCE PRINCIPLE TO CONSTANT-STRAIN-RATE MONOTONIC LOADING

A series of uniaxial tensile tests was performed on the asphalt concrete specimen at 25°C at different constant strain rates ranging from 0,0001 units/sec to 0,0032 units/sec as presented in table 3.

Figure 8 displays the rate-dependent behaviour observed from the asphalt mixture under study.

As mentioned before, the application of the correspondence principle calls for the calculation of pseudo strain ε^R. Now, the test results shown in figure 8 are represented in terms of pseudo strain in figure 9. The pseudo strain, according to equation 2 with the use of equation 12, is given by

$$\varepsilon^R = R/E_R \left(E_\infty t + \sum_{i=1}^{N} E_i \rho_i \left(1 - e^{-t/\rho_i}\right)\right) \quad (13)$$

where R is the constant strain rate and t is time that can be computed by $t = \varepsilon/R$ in this case of a constant strain rate. The reference modulus $1/E_R$ was taken to be equal to the initial modulus of 3,14627E-07 kPa^{-1} corresponding to t = 0.

In figure 9, pseudo strains were plotted against σ/I. The initial pseudo stiffness, I, defined as the ratio of stress to pseudo strain at the early linear part of a stress-pseudo strain curve, was necessary to account for the effect of sample to sample variability.

From figure 9 it is evident that the curves representing different loading rates fall on approximately the same line at lower stress levels, and then the discrepancy becomes greater. This is particularly true for the higher strain rates,
R = 0,0016 units/sec and
R = 0,0032 units/sec.

This behaviour implies that the correspondence principle can successfully eliminate the rate dependency of the material at low stress and strain levels.

CONSTITUTIVE MODEL CHARACTERISATION

Uniaxial viscoelastic damage model for asphalt concrete

A simple constitutive model for uniaxial stress-strain behaviour of asphalt concrete with time-dependent damage growth was proposed as follows (Park *et al* 1996):

First, for the pseudo strain energy density function of the material, the simplest possible form is

$$W^R = \frac{1}{2} C(S)(\varepsilon^R)^2 \quad (14)$$

where the coefficient C is a function of a single damage parameter S.

*Table 3 Constant-strain-rate monotonic loading**

Number	Mode	Wave form	Strain amplitude (units/sec)
1	Uniaxial tensile	Haversine	0,0001
2	Uniaxial tensile	Haversine	0,0004
3	Uniaxial tensile	Haversine	0,0016
4	Uniaxial tensile	Haversine	0,0032

* All four tests at different strain amplitudes were performed on the same specimen (diameter: 100 mm, height: 110 mm), allowing a 40-minute rest period between the tests. Stress-versus-strain behaviour at different strain rates is depicted in figure 8.

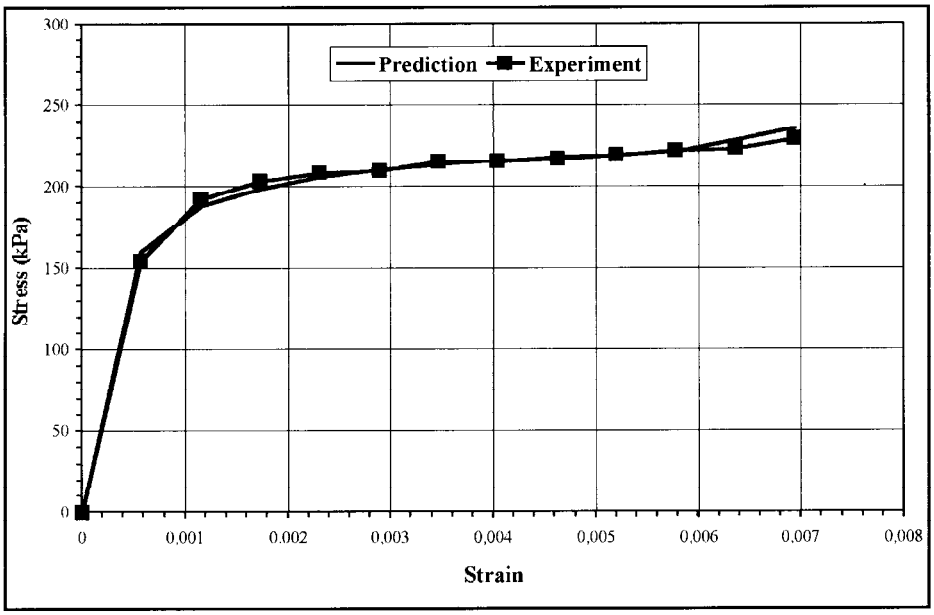

Figure 10 Stress prediction laboratory tests vs constitutive model for R = 0,0001 units/sec

Then

$$\sigma \equiv \frac{\partial W^R}{\partial \varepsilon^R} = C(S)\varepsilon^R \qquad (15)$$

which, for fixed damage, is an equation for linear viscoelastic behaviour. The damage evolution law is the following single equation for S:

$$\dot{S} = \left(-\frac{\partial W^R}{\partial S}\right)^{\alpha} \qquad (16)$$

Equations 14–16 constitute a model for the uniaxial stress-strain behaviour of a viscoelastic solid (asphalt concrete, in this case) with time-dependent damage growth.

The form of equation 16 is consistent with the behaviour of the stress versus pseudo strain curves presented in figure 9. The figure indicates that stress is linearly proportional to pseudo strain at low strain levels where practically no damage has occurred. This situation corresponds to a constant value of the constitutive function C in equation 15 and thus results in a linear relationship between σ and ε^R. As pseudo strain level increases, each curve deviates from the linear relationship indicating a reduction of C, so that $dC/dS \leq 0$.

Interestingly, each curve in figure 9 bends at a different rate for a given pseudo strain level, suggesting that the damage growth is not only rate-dependent through ε^R, but also exhibits additional rate dependence. Lower strain-rate curves bend at lower ε^R, indicating that more damage occurs at longer loading durations for the same pseudo strain. This behaviour is consistent with equation 16. The evolution law equation 16 reflects rate-effects through ε^R in W^R and explicit time-effects through the time derivative of S on the left-hand side.

Therefore, the only damage-related constitutive parameters to be determined to develop a uniaxial viscoelastic damage model for asphalt concrete are the functions $C(S)$ and the constant α.

In order to find the function $C(S)$, first the value of C is obtained by fitting equation 15 to an experimental stress-pseudo strain curve with R = 0,0001 units/sec. This process determines a modulus C that depends on ε^R and strain rate, but not S directly. In order to find its dependence on S alone, it is necessary to find a relationship between S, ε^R and rate (or time). Finding this relationship requires the use of the postulated evolution law. However, the rate-type evolution law equation 16 is not adequate for finding S directly for a given ε^R because the equation itself requires *a priori* knowledge of the functional form of $C(S)$ before the equation can be solved for S; the solution of S for the given ε^R would require an extensive iteration process which would be highly impractical. To overcome this problem, an approximation procedure developed by Schapery (1990) was used.

The constant α needs to be known a priori; however, a reasonable initial guess for α can be done on the basis of the linear viscoelastic fracture mechanics.

In many viscoelastic crack growth problems, the crack speed is governed by the α^{th} power in pseudo energy release rate, in which α is related to the material's creep or relaxation properties. For example, $\alpha = 1 + 1/n$, in which n = logD(t)/log(t) or n = – logE(t)/log(t) at times depending on crack speed, which was shown by Schapery (1975, part III) for rubber.

It is assumed that the damage that occurs in the specimen is closely related to the growth of microcracks.

The relationship $\alpha = 1 + 1/n$ was used in this instance. An initial value of 2,5 was adopted for α based on n = 0,65, which is the value of slope obtained from the master creep compliance curve, as depicted in figure 3. By trial and error, it was found that with α = 2,35, the model predicts the experimental observations most closely.

The resulting functional form for $C(S)$ is

$$C = 958879 \times S^{-0,4044} \qquad (17)$$

Prediction of mechanical response and damage evolution

Having found the constitutive parameters employed in the model, it is possible now to predict the stress for a given strain history.

First, the pseudo strain ε^R is computed according to equation 13. The damage parameter S was obtained from equations 16 and 14 through a summation of the increments of S ($\Delta S = \dot{S}\Delta t$ over the time elapsed, with an initial condition of $S = 0$ at $t = 0$). Finally, the stress was predicted by using equation 15.

Figure 10 depicts the stress prediction based on the strain history for a constant strain rate of 0,0001 units/sec.

The curve for R = 0,0001 units/sec is in good agreement with its experimental data. Nevertheless, it should be borne in mind that this experimental data was used in the characterisation of the model.

FATIGUE PREDICTION CURVES

Three different fatigue curves are discussed in this section. Firstly, a laboratory curve was determined, based on the third-point loading fatigue testing programme carried out at the CSIR Transportek laboratories. Secondly, a conventional fatigue crack initiation transfer function for continuously graded asphalt was used to develop a fatigue curve based on the South African Mechanistic Design Method. Finally, a third curve was derived, based on the constitutive modelling approach.

The derivation of the laboratory curve, as shown in figure 13, was based on the use of the third-point loading fatigue tests and the determination of the

Table 4 Characteristics of third-point loading fatigue testing

Beam (No)	Temperature (°C)	Frequency (Hz)	Strain level	E initial (MPa)	E failure (MPa)	Fat. Life (repet)
1	5	10	534	9 479	4 739,5	19 998
2	5	10	349	10 472	5 236	89 998

Table 5 Constant-strain cyclic loading test

Strain amp	Mode	No of cycles	Wave form	Loading rate
0,0007	Uniaxial tensile	Up to failure	Haversine	1,0 sec/cycle
0,0014	Uniaxial tensile	Up to failure	Haversine	1,0 sec/cycle

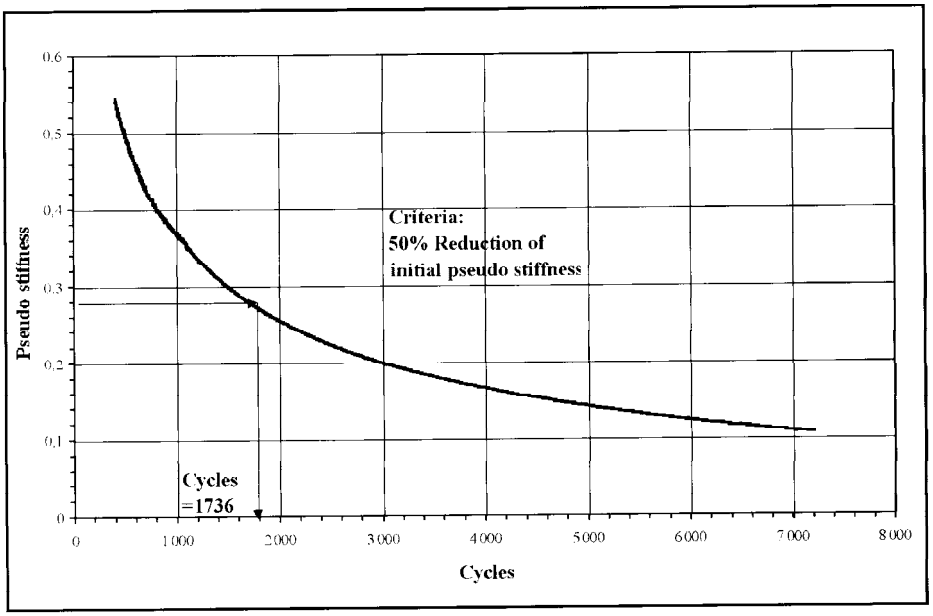

Figure 11 Pseudo stiffness versus number of cycles for 0,0007 strain amplitude

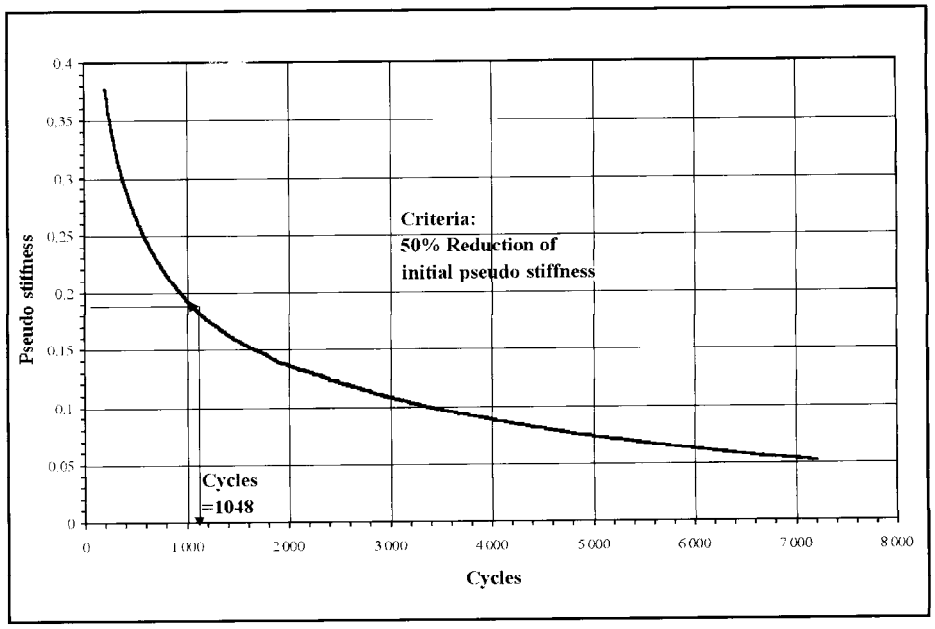

Figure 12 Pseudo stiffness versus number of cycles for 0,0014 strain amplitude

fatigue failure point as the number of load repetitions to a 50% reduction in the initial stiffness value.

This laboratory curve was developed by using the two tests performed on the specimens at different controlled deflections, which correspond to different controlled strains, as summarised in table 4. The fatigue characteristics of asphalt mixtures are usually expressed as a relationship between initial stress or strain and number of load repetitions to failure. A fatigue curve in the form of initial strain versus number of load applications was then developed.

In order to compare the conventional methodology to the one proposed in this study, the fatigue curve for continuously graded asphalt for category A roads (Jordaan 1993) is also depicted in figure 13.

The predicted curve using the constitutive model was derived as follows: Two constant-strain cyclic loading tests were performed at the CSIR laboratories and their characteristics are summarised in table 5. The pseudo strains were calculated using equation 13 for both tests.

Now, to predict the fatigue life of the mixture using the constitutive equation a failure criterion is required. A traditional failure criterion, 50% of the initial stiffness, can be used, as was done with the laboratory curve based on the third-point loading fatigue tests. However, in this case a 50% reduction in the initial pseudo stiffness was used as a failure criterion. Pseudo stiffness was calculated by dividing stresses measured during the tests by the pseudo strains as obtained from equation 13. The first 400 and 200 cycles were discarded to allow for the initial test conditions to reach equilibrium for 0,0007 and 0,0014 strain amplitudes, respectively. Figures 11 and 12 show the calculation of the number of cycles to fatigue failure for the 50% reduction in pseudo stiffness, used as failure criterion. Finally, the predicted curve is depicted in figure 13.

A functional form of N_f-ε was obtained by means of curve fitting for the different prediction curves. The results are summarised in table 6. The reference temperature is different for the various curves, reflecting the different laboratory test conditions.

As expected, all three curves depicted in figure 13 show a decrease in the number of cycles to fatigue failure with an increase in the magnitude of tensile strain.

Both the South African Mechanistic Design Method curve and the Third-Point Loading Fatigue Test curve (SAMDM curve and laboratory curve) show a rapid decrease in the number of cycles to fatigue failure with an increase in tensile strain, particularly in the former.
It should be remembered that the transfer function used in the SAMDM curve was developed considering that the number of load repetitions to failure represents the number of repetitions to the point of crack initiation in the asphalt layer. A fatigue crack propagation shift factor of 10 for an asphalt layer thickness of 200 mm is typically used to convert laboratory life to field life (Jordaan 1993).

In the case of the laboratory curve, the controlled-strain approach was followed; as the controlled-strain fatigue test progresses, the deflection remains constant up to the point of initial crack failure and then decreases until complete failure. For low deflections there is a substantial difference in the number of repetitions to the initial failure point and the ultimate failure of the specimen, which makes the determination of the exact number of repetitions to the initial crack stage sometimes difficult. A failure criterion of 50% reduction in the initial stiff-

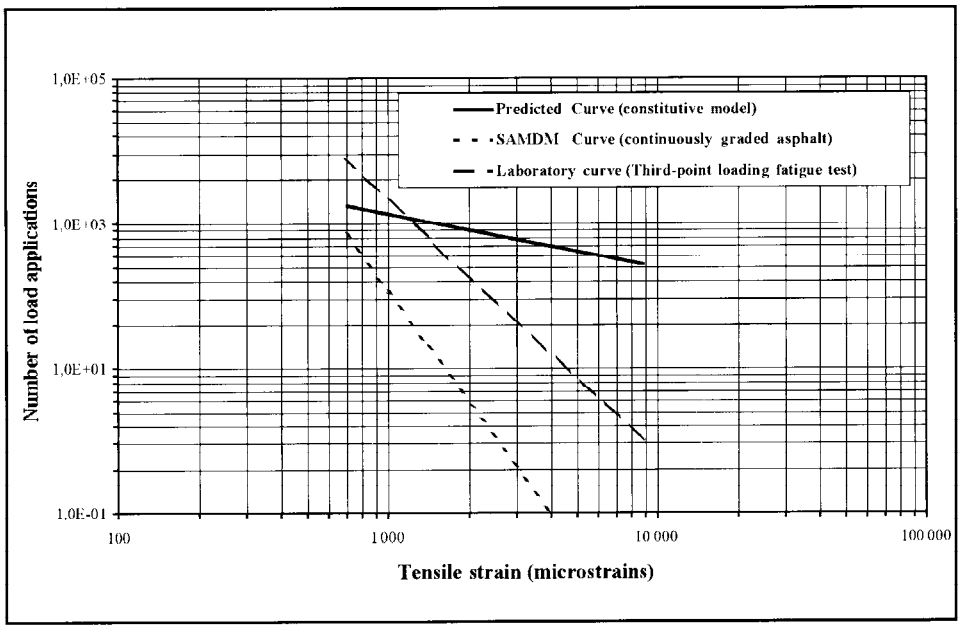

Figure 13 Fatigue prediction curves - number of load applications to failure N_f versus tensile strain ε

Table 6 Fatigue prediction curves functional forms

Description	Functional form	Temperature (°C)
Predicted curve (constitutive model)	$N_f = 10^{3,60(1-\frac{Log\ \varepsilon}{6,20})}$	25
SAMDM curve (cont. graded asphalt)	$N_f = 10^{17,40(1-\frac{Log\ \varepsilon}{3,40})}$	20
Laboratory curve (third-point loading test)	$N_f = 10^{4,64(1-\frac{Log\ \varepsilon}{37,69})}$	5

ness value was considered for the controlled-strain fatigue tests. Nevertheless, N_f represents the number of load repetitions to laboratory fatigue test failure and therefore there is a slight amount of crack propagation included in the N_f fatigue curve (Airey & Visser 1997).

The constitutive model curve presents a smaller slope compared to the other two curves, consequently less sensitive to increases in the tensile strain values. Within the range of tensile strains analysed, the constitutive model curve presents higher values of number of repetitions to failure than the other two curves. It must be remembered that only one temperature was used in the fatigue testing (T = 5°C). It is accepted that there is a decrease in stiffness (and consequently in the number of load repetitions to fatigue failure, N_f) as the testing temperature increases. This decrease in stiffness is a result of the viscoelastic asphalt mixture having an increased viscous (flow) behaviour at elevated temperatures.

CONCLUSIONS

A methodology capable of predicting the fatigue performance of asphalt concrete considering damage evolution was introduced in this study and the correspondence principle developed by Schapery (1984) was validated for a continuously graded asphalt mix. The correspondence principle calls for the calculation of pseudo strains and, in turn, the expression of a relaxation modulus is required for the calculation of pseudo strains. The approach followed in the present study was to predict the relaxation modulus from a simpler test, such as the creep test. The master creep compliance curve was derived, and with the use of a Prony series representation, both the master creep compliance and the master relaxation curves were obtained. Then, the correspondence principle was applied to constant-strain-rate monotonic loading tests and it was proved that this principle can effectively eliminate the rate dependency of the material.

It was also shown that the dependence of asphalt concrete to both time and temperature can be represented by the dependence on a single variable, the reduced time defined by equation 8. This feature is referred to as time-temperature superposition and was applied to a series of creep curves obtained at different temperatures in order to derive a master creep compliance curve by using the time-temperature shift factors aT given in figure 5.

A method for Prony series representation was presented. The experimental data with scatter were smoothed using a power-law series representation, and then a Prony series expression of the material function was determined by fitting it to the pre-smoothed data. The impact of random errors in the source data on the resulting Prony series was minimised by pre-smoothing. Pre-smoothing the data enhances the consistency of the data and eliminates the local waviness in the reconstructed curves (Park & Kim 1999).

Furthermore, a simple constitutive model for uniaxial stress-strain behaviour of asphalt concrete with time-dependent damage growth was proposed and the damage-related constitutive parameters, the function $C(S)$ and the constant α were determined. Having found the constitutive parameters employed in the model, the stress for a given strain history was predicted as shown in figure 10.

Fatigue performance was studied by developing three different fatigue curves. Firstly, a laboratory curve was determined based on the third-point loading fatigue testing programme carried out at the CSIR laboratories. Secondly, a conventional fatigue crack initiation transfer function for continuously graded asphalt was used to develop a fatigue curve based on the South African Mechanistic Design Method. Finally, a third curve was derived based on the constitutive modelling approach. It should be noted that the curves were derived for different temperatures. It was found that the constitutive model curve presents a smaller slope compared to the other two curves, consequently less sensitive to increases in the tensile strain values. Within the range of tensile strains analysed, the constitutive model curve presents higher values of number of repetitions to failure than the other two curves. This curve should be considered as a first attempt to obtain an alternative characterisation of asphalt concrete to fatigue behaviour. Overall, the approach presented in this study has proved to be an important tool to accurately describe asphalt concrete behaviour. It is also important to put in place a more comprehensive testing programme to evaluate asphalt concrete response to fatigue within a wider range of tensile strains as well as further explore the extrapolation used in this paper between constant-strain-rate monotonic loading and constant-strain cyclic loading.

Acknowledgements

- The Southern African Bitumen Association (SABITA) for funding the laboratory test programme used in the MEng project report.
- The CSIR Transportek Division Laboratories for carrying out the test programme.

References

Airey, G D & Visser, A T 1997. Development of the third-point loading fatigue test and fatigue curves for LAMBS. *SAICE Journal*, 39(1):1–5.

Ferry, J D 1980. *Viscoelastic properties of polymers*. University of Wisconsin, USA.

Jordaan, G J 1993. *Users manual for the South African Mechanistic Pavement Rehabilitation*

Design Method. Report Nr IR91/242. Department of Transport, Pretoria, South Africa.

Kim, Y R, Lee, Y & Lee, H J 1995. Correspondence principle for characterization of asphalt concrete. *Journal of Materials in Civil Engineering,* ASCE, 7(1).

Kim, Y R, Lee, H J & Little, D N 1996. *Fatigue Characterization of Asphalt Concrete Using Viscoelastic and Continuum Damage Theory.* Association of Asphalt Paving Technologists, USA.

Lytton, R L, Uzan, J, Fernando, E G, Roque, R, Hiltunen, D & Stoffels, S M 1993. *Development and validation of performance prediction models and specifications for asphalt binders and paving mixes.* Strategic Highway Research Program. Report A-357. National Research Council. Washington DC, USA.

Park, S W, Kim, Y R & Schapery, R A 1996. *A viscoelastic continuum damage model and its application to uniaxial behaviour of asphalt concrete.* Civil Engineering Department, North Carolina State University, USA.

Park, S W & Kim, Y R 1999. *Prony series representation of viscoelastic material functions with power-law pre-smoothing.* Civil Engineering Department, North Carolina State University, USA.

Schapery, R A 1975. A theory of crack initiation and growth in viscoelastic media. Part I: Theoretical development; Part II: Approximate methods of analysis; Part III: Analysis of continuous growth. *Int J Fract,* 11:141–159, 369–388, 549–562.

Schapery, R A 1984. *Correspondence principles and a generalized integral for large deformation and fracture analysis of viscoelastic media.* Civil Engineering Department, Texas A&M University, USA.

Schapery, R A 1990. A theory of mechanical behavior of elastic media with growing damage and other changes in structure. *J Mech Phys Solids,* USA.

TRH4 1996. Technical recommendations for highways. *Structural design of flexible pavements for interurban and rural roads.* Department of Transport, Pretoria, South Africa.